EMERGENT: JOURNAL OF EDUCATIONAL DISCOVERIES AND LIFELONG LEARNING (EJEDL)
ISSN: 2776-0995 Volume 7, Issue 5 May- 2026

MULTI-ILLUMINATION OPTICAL DESCRIPTORS IN DUAL-BRANCH SVM APPROACH IN CLASSIFYING EDGES OF MATERIALS DEPLOYED ON EDGES

Palvannazirova Nasiba
School of Electronic Engineering
BUPT, line 3:Beijing, China
nasiba@bupt.edu.cn

Butovskiy Petr
Technological Machines and Apparatus
TITLI, Tashkent , Uzbekistan
* Corresponding author: gtnz1071980@gmail.com

Ayaz Waseem
School of Electronic Engineering
BUPT, line 3:Beijing, China
2024090002@bupt.cn

Mavlyanov Aybek
Technological Machines and Apparatus
TITLI, Tashkent , Uzbekistan
mavlyanov@gmail.com

Abstract

The issue of automated fabric recognition in the textile manufacturing industry is still a challenge because it is difficult to differentiate between substances of the same appearance yet having different physical characteristics. Whereas the weave patterns can be determined with the help of the geometric analysis, the recognition of the material composition demands more advanced techniques. The current paper introduces a biomimetic visual analysis system based on the processes of human experts inspection. We suggest a two-branch model in which the analysis of the geometric structure is mixed with multi-oriented- illumination- optical feature extraction. With the help of controlled lighting conditions, i.e. direct, angled (45deg), and backlight illumination, we pull out a set of specular reflection maps, surface roughness indices, as well as light absorption coefficients which are effective in distinguishing between natural and synthetic fibers. Our approach manages to identify materials with accuracy of 87.3% in cotton, polyester, silk and blended fabrics when geometry is used compared to 64.2% in geometry only. The system is based on edge computing hardware (ESP32-CAM), which allows connecting in real-time with industrial sewing machines. It is experimentally validated by using 1,200 samples of fabric, which shows good performance in different colors and densities of weaves. The

given strategy fills the gap between the human-like perception of reasoning and the automated quality control in textile manufacturing.

Keywords: Fabric recognition; computer vision; optical analysis; edge computing; biomimetic systems; textile manufacturing.

I.INTRODUCTION

Textile business is facing an increasing need to apply automated quality control and molding manufacturing systems. One of the essential issues is correct fabric identification, i.e. identification of not only the features of structure (pattern of weave, density of threads, etc.), but also the composition (cotton, polyester, mixed fibers, etc.). This task can be realistically carried out by the experienced textile technologists with ease by providing visual and tactile check, but when dealing with the materials, which are similar based on the common imaging conditions, the automated systems suffer [1], [2].

The ancient methods of computer vision used in the fabric analysis are mostly based on the use of the texture descriptors and geometric features extraction [3], [4]. The methods are very effective in detecting patterns of the weave, plain, twill, and satin weaving, using spatial frequency analysis, and directional gradient histograms. They however end up falling short when faced with the question of a basic problem of differentiating blue cotton and blue polyester. The two fabrics can be of the same weave pattern and even have the same colors distribution however the fabrics must have completely different processing parameters in manufacturing.

This is a problem that is solved by human experts using multi-modal inspection i.e. looking at the reflections of light on the faces of fiber and being aware of the typical plastic-sheen coloration of artificial material as opposed to the matte look of natural material, and comparing the subtle changes in texture that can be seen in multiluminated photography. The implicit conception of material optical characteristics, including diffuse and specular reflection, roughness of surface and light absorption is all included in this perceptual process [5].

The recent deep learning strategies demonstrated impressive performances in the matter of fabric classification [6], [7], but most of them are black boxes, which is not explicitly modeled after the physical mechanisms that determine human perception. Moreover, the techniques are usually very computational intensive, so they cannot be applied in edge computing applications that are widespread in industrial applications.

The presented paper forms a biomimetic strategy that literally simulates human visual inspection using the multi-scale optical analysis. The main points that we would make are:

1) The geometrical structure analysis and material specific optical features extraction have been segregated in a dual branch architecture.
2) New optical factors of multi-illumination imaging: index of specularity, surface roughness, and directional absorption.
3) Phases Underlying mathematical derivation of pixel measures of materials as a first-principles derivation of physical material properties.
4) Real-time application based on ESP32-CAM microcontroller platform which proved to be viable in terms of real-time industrial implementations.

In the rest of this paper, the data will be structured in the following fashion: Section II does the literature review. Section III is a presentation of methodology. Section IV entails experiment set-up. The results are given in section V. In section VI implications are discussed. Section VII concludes.

II. RELATED WORK

A. The analyses of Geometric fabrics.

The geometrical texture measures are put into consideration by the classic computer vision approaches to fabric analysis. The layout of the spatial connection among pixel values and, thus, distinguish patterns of reverted weave structures are represented by the Gray-Level Co-occurrence Matrices [8] and Local Binary Patterns [9]. Frequency domain techniques are also frequency domain methods that are used to define the density of threads and weave periodicity such as Fourier transform techniques [10], [11]. These techniques are used in order to provide the effective means of classifying the structures but little information on the materials composition.

B. Deep Learning in the case of Fabric recognition.

In the recent times, it has made use of the convolutional neural network in fabric classification. It is proven in the literature that: transfer learning with using pre-trained models (VGG, ResNet) is highly accuracy on benchmark datasets [12], [13]. Nevertheless, these methods usually have thousands of training samples, and they are not interpretable as to what visual characteristics are capable of causing classification decisions. Other vision transformers [14] are also appealing, although this involves much computation which is hard to fit on the edge.

C. Analyses of Optical Material

Computer graphics [15], [16] and robotics [17] have also studied computer graphics using the optical property of a material. The idea of reflectance analysis or material differentiation is pegged on the bidirectional reflectance distribution functions (BRDF) of a material. Multi-illumination imaging is the description of an object that is done under different lights so that the inferences can be made concerning the properties on the surface [18], [19]. But structured application of such techniques has not been

EMERGENT: JOURNAL OF EDUCATIONAL DISCOVERIES AND LIFELONG LEARNING (EJEDL)
ISSN: 2776-0995 Volume 7, Issue 5 May- 2026

applied to textile materials that have special challenges because of anisotropic fibre structures and complicated light scattering behaviour.

D. Image computing of factory vision.

The development of edge computing platforms can be used on-machine learning in factories [20], [21]. ESP32 systems possess low level of power consumption and contain sufficient processing units that can process images in real time [22]. Most of the tasks are focused on the detection of defects and not the sorting of materials although the recent practice demonstrates that lightweight neural networks can be implemented in quality inspection tasks successfully [23].

III. METHODOLOGY

The suggested system represents fabric inspection as a multi-scale hierarchical multi-level perceptual process: in the structural pattern recognition, geometric weave analysis, and material-discriminate optical evaluation. All the fabric samples are photographed at four defined illumination conditions, and parallel feature branches are used to process the images obtained prior to fusion and SVM classification.

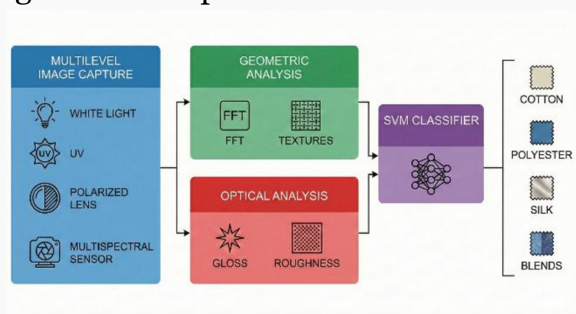

Figure 1. Whole system architecture relating to multi-illumination capture, dual-branch feature extraction and fusion classification. The optical branch characterizes the information that can be obtained in the structure of the weave; the geometric branch characterizes the material specific reflectance properties.

Multi-Illumination Image Acquisition.

It uses four sequential illumination conditions which are used to show complementary physical properties. Ambient illumination (I_{amb}) is used to set a colorimetric baseline at diffuse light but when all LEDs are put off. Direct illumination (I_{dir}) has the LED coaxial to the camera and is used to inhibit the specular return and is the main source of geometric analysis. The slice of illumination (I_{ang}) in the 45° direction relative to the surface normal preferentially excites the specular reflection, smooth synthetic fibers result in focused highlights, matte natural fibers give diffuse returns, and the difference between I_{ang} and I_{dir} forms the basis of the measurement of the specularity index in Section III-C. Backlight illumination (I_{back}) attenuated as it penetrates the thickness of.

EMERGENT: JOURNAL OF EDUCATIONAL DISCOVERIES AND LIFELONG LEARNING (EJEDL)
ISSN: 2776-0995 Volume 7, Issue 5 May- 2026

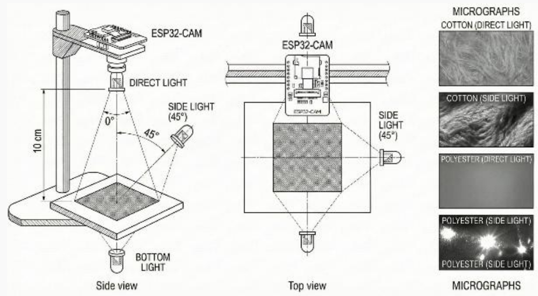

Figure 2. Figure of the four light setups (ambient, direct, angled 45°, and a backlight) and sample images of cotton and polyester in each set up.

Geometric Feature Extraction

- The geometric branch works based on the I_{dir} which has coaxial illumination geometry that eliminates directional reflectance artifact and gives spatially homogeneous excitation appropriate to structural analysis. Fabric weave has takes the form of quasi-periodic space arrangements; Discrete Fourier Transform separates these into frequency space components:

$$F(u,v) = \frac{1}{MN} \sum_{x=0}^{M-1} \sum_{y=0}^{N-1} I_{dir}(x,y) e^{-2\pi i (\frac{ux}{M} + \frac{uy}{N})} \qquad (1)$$

- Its power spectrum of $P(u,v) = |F(u,v)|^2$ directly gives the periodicities to which density of threads rho is directly retrieved:

$$\rho = f_p * r \qquad (2)$$

- Where peak frequency f_p and resolution of the imaging r (pixels/cm). Weave distribution Can be determined by the angular component of spectral energy:

$$E(\theta) = \sum_r P(r\cos\theta, r\sin\theta) \qquad (3)$$

- Plain weave will give sharp peaks at $\theta = 0$ and 90° degrees, twill will give lobes of a diagonal shape at $\pm 45^\circ$ or $\pm 60^\circ$ and satin will give a wide diffuse spectrum. In order to resolve fine-scale irregularities that spectral analysis does not, Local Binary Pattern (LBP) codes are calculated at every pixel (x_c, y_c) over P neighbours at radius R:

$$LBP_{P,R}(x_c, y_c) = \sum_{p=0}^{P-1} s(g_p - g_c) * 2^p \qquad (4)$$

- and g_c and g_p are the pixel intensities of the center and neighbor respectively, and s(•) is the unit step function.

The normalized LBP histogram is physically significant and rotation-invariant: natural fibers have large variances due to the natural cross-sectional flatteness, and extruded synthetic fibers have small variances due to the compactness of their distributions.

ISSN: 2776-0995 Volume 7, Issue 5 May- 2026

Optical Feature Extraction

The optical division is concerned with the fundamental flaw of wholly geometrical methods the failure to differentiate between fabrics with the same weave but made of different fibers. It describes the light-matter interaction in the illumination set, the strategy of the trained textile technologists to use in the multi-angle inspection.The intensity that is reflected at individual points on each surface is assumed to be the sum of Lambertian diffuse and Phong specular components:

$$I_{ref}(x,y) = k_d * L * \cos\theta_i + k_s * L * (\cos\alpha)^n \qquad (5)$$

k_d and k_s are the specular and diffuse reflection coefficients, the incidence angle is denoted as θ_i and the angle between the specular and the viewing angles is denoted as α and the shininess parameter n used in Phong is denoted as n. These parameters are diagnostic per se: synthetic fibers are those with $k_s > 0.3$ and $n > 20$; the ones with natural fibers are those with $k_s < 0.1$ and $n < 5$.

The Specularity Index (SI) takes advantage of the difference between the coaxial and angled light. Direct illumination $\alpha \approx 90^{\circ}$ pushes the specular return to its lowest, and angled illumination 45° draws 0° specular highlights on smooth synthetic surfaces. This modulation is isolated with the pixel-wise difference, $S(x,y) = I_{ang}(x,y) - I_{dir}(x,y)$, and the sum of this modulation is normalized by the brightness, SI:

$$SI = \frac{1}{MN * \sigma_I} \sum_{x=1}^{M} \sum_{y=1}^{N} \max(S(x,y),0) \quad (6)$$

In which σ I is a normalization of the total brightness in a scene, and the max(, 0) operation eliminates adverse values of registration noise. Experimentally determined calibration values of polyester include SI >2.5; cotton, SI <1.2; and between these values of mixed compositions.

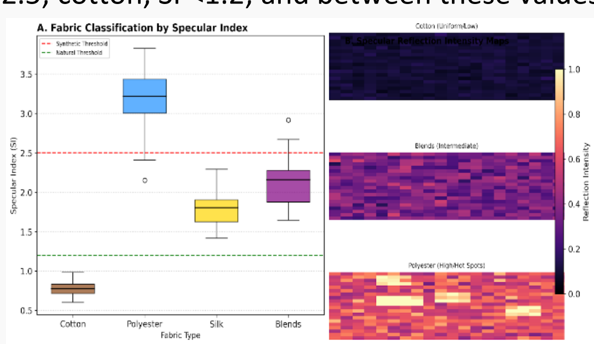

Figure 3. Index of specularity of the various types of fibers. Figure (a) Box plots with a distinct cut off between material classes. Example specularity maps 2 S(x,y) of cotton, polyester and mixed samples, showing center of focus intensity in synthetic fabrics, and diffusive nature in natural ones.

The Surface Roughness Coefficient (RC) is an image product of backlights. Transmittance: Beer-Lambert attenuation $I_{back}(x,y) = L_0 e^{-\mu t(x,y)}$. A sliding window of $w*w$ sizes computes local intensity variance $V_{local}(x,y)$ which RC sums up on a global basis:

$$RC = \frac{1}{MN}\sum_{x=1}^{M}\sum_{y=1}^{N} V_{local}(x,y) \qquad (7)$$

Cotton yields RC = 850-1200 and linen RC = 1100-1500, capture surface fibrils and irregular cross-sections and polyester is 200-400 which is smooth extruded geometry. RC therefore gives a discrimination axis which is normal to SI.

The approximation of the light absorption is based on the log-ratio of the direct illumination to a white diffuse reference I_{ref}

$$\alpha(x,y) = -\log\left(\frac{I_{dir}(x,y)}{I_{ref}}\right) \qquad (8)$$

The absorption map is summarized by two statistics; mean absorbance and spatial variance:

$$\overline{\alpha} = \frac{1}{MN}\sum_{x=1}^{M}\sum_{y=1}^{N}\alpha(x,y) \qquad (9)$$

$$\sigma_\alpha^2 = \frac{1}{MN}\sum_{x=1}^{M}\sum_{y=1}^{N}\left[\alpha(x,y) - \overline{\alpha}\right]^2 \qquad (10)$$

The non-uniform absorption of reactive dyes on cotton is caused by the uneven crystallinity of fibers and accessibility of hydroxyl groups, and gives large σ_α^2. Homogenous uptake and resultantly low σ_α^2 is given by polyester that is dyed under high temperature through disperse dye diffusion.

Fusion of the Features and Classification

The feature vector of the two branches is summed together:

$$F = \left[f_{geom}, f_{opt}\right] \qquad (11)$$

- $f_{geom} = \left[\rho_h, \rho_v, E_\theta, LBP_{hist}\right], f_{opt} = \left[SI, RC, \overline{\alpha}, \sigma_\alpha\right]$. The classification is done after the normalization of all features to zero mean and unit variance.
- F: is trained with an SVM using RBF kernel:

EMERGENT: JOURNAL OF EDUCATIONAL DISCOVERIES AND LIFELONG LEARNING (EJEDL)
ISSN: 2776-0995 Volume 7, Issue 5 May- 2026

$$K(F_i, F_j) = \exp(-\gamma \|F_i - F_j\|^2), \gamma = 0.1 \quad (12)$$

- with 5-fold cross-validation 5-fold cross-validation of γ . It is classified by a one-versus-rest scheme; the classifier with the largest signed decision value is the one that has been predicted to be the correct one:

$$y_c(F) = sign(\sum_{i=1}^{N_s} \alpha_i y_i K(F_i, F) + b) \quad (13)$$

- In which α_i are the learned Lagrange multipliers and b the bias term. It is the choice of SVM because it has been shown to perform effectively in moderate dimensionality feature space, has a built-in margin-based boundary, and gives per-feature importance weights that can be readily interpreted - a liability that makes it pragmatic in industrial fault diagnosis.

Experimental Setup

Hardware Configuration

The camera is constructed on the ESP32-CAM platform with the help of an OV2640 image sensor (16001200), intended to be inverted and mounted 10 cm over the fabric stage. Such geometry provides the effective resolution of around 0.05 mm/pixel, which is good enough to distinguish between the points of the yarn interlacing. There are four illumination conditions (that are independently switchable) with three white LEDs (5000 K color temperature, 5 W each) which are coaxially aligned with the camera optical axis, 45 degrees to the surface normal, and below a transparent acrylic stage where the illuminated area can be contaminated by the light. Raspberry Pi 4B (4 GB RAM) is used to extract features and classify them, and then it can communicate with ESP32-CAM through WiFi. The entire set is housed within a light regulated compartment to destroy ambient lighting inconsistency in the process of taking the picture. The hardware modeling of the system is presented in Fig. 4.

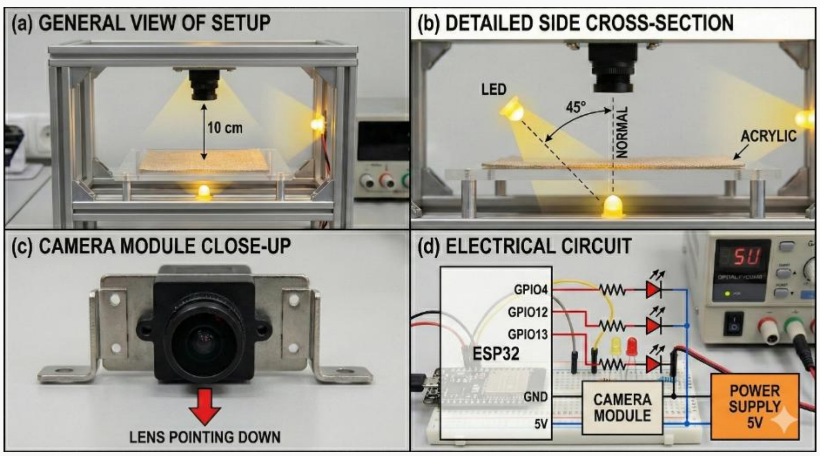

Figure 4. Combination of the multi-illumination capture system with physical implementation. Figure 1 (a) The overall picture of the entire assembly with the camera placed at a height of 10 cm above the fabric stage. (b) Cross-section of the details of the 45 o LED angle with respect to the surface normal and through the transparent backlight stage of acrylic. (c) Close-up ESP32-CAM module with a lens, which is aimed at fabric image reading. As seen in electrical circuit schematic (d), LED is controlled by using ESP32 GPIO pins (GPIO4, GPIO12, GPIO13); this involves connecting this LED to ESP32 5 V power supply.

EMERGENT: JOURNAL OF EDUCATIONAL DISCOVERIES AND LIFELONG LEARNING (EJEDL)
ISSN: 2776-0995 Volume 7, Issue 5 May- 2026

Dataset

Fabric samples of four types of materials were sampled including, cotton with (n = 8), polyester with (n = 7), silk with (n = 5), and silk as a blended cotton-polyester (50/50) with (n = 6). Individual categories consist of various colorways so that the differentiation of materials is learnt regardless of color. To capture the 26 samples, 10 spatially different regions had been imaged with each four different illumination conditions (10 imaging points per region and 40,000 images per sample). The composition of datasets was outlined in Table I.

TABLE I. MATERIAL-TYPE DATASET COMPOSITION

Material	MATERIAL-Type Dataset Composition.		
	Samples	Images	Color Distribution
Cotton	8	3200	White (2), Blue (2), Red (1), Green (1), Black (1), Striped (1)
Polyester	7	2800	White (1), Blue (2), Black (2), Purple (1), Patterned (1)
Silk	5	2000	White (1), Cream (1), Pink (1), Gold (1), Burgundy (1)
Blended (50/50)	6	2400	White (2), Blue (1), Gray (1), Beige (1), Checked (1)
Total	26	10400	

Partitioning of data occurred at sample level rather than image level in such a way that data in different splits is not leaked; 18 samples ((6,480 images) to train, 4 samples (1440 images) to validate and 4 samples (1440 images) to test. This will guarantee the classifier a sample of fabric that will be actually non-observed.

Implementation

The fourier transform with NumPy FFT was used to extract features in the OpenCV 4.6 and the standard LBP implementation was performed with $P=8$ neighbors $R=1$. Computations of specularity and roughness are done in a 5×5 pixel sliding window. The time per sample (four images), including a total of 280 ms, is within the range of allowing a real-time application.

SVM training used scikit-learn 1.1.2 with an RBF kernel ($C=10, \gamma=0.1$). All the features were brought to zero mean and unit variance before the process of training. The choice of hyperparameters was done through 5-fold cross-validation on the training division; the training time on a typical desktop (Intel i7, 16 GB RAM) is about 45 seconds.

Results and Discussion

Classification Performance

Table II shows classification accuracy when using various features setups. The complete biomimetic model exhibits 87.3 test accuracy which is significantly higher than that of the geometry only baseline (64.2) and color only baseline (58.7). Interestingly, organic features that can be captured by optical features alone (76.5%), rather than geometric features (64.2%), confirm that material discrete reflectances have more discriminative information than their structural characters in separating similar weave fabrics of different fiber composition.

TABLE II. ACCURACY OF CLASSIFICATION OF VARIOUS FEATURE COMBINATIONS

Accuracy of Classification of various feature combinations		
Feature Set	**Validation**	**Test**
Geometric only (FFT + LBP)	67.8%	64.2%
Color features (HSV histograms)	61.2%	58.7%
Geometric + Color	72.5%	69.8%
Optical only (SI + RC + Absorption)	79.3%	76.5%
Full Model (Geometric + Optical)	89.6%	87.3%

This confusion matrix of the complete model, per-class, is depicted in Fig. 5. Cotton and polyester have a close percentage of recall repeat of 96 and 94 percent respectively separating them as a highlighting index indicating the discriminatory quality of specularity index to be an advantageous grouping among natural and artificial fibers. Classification of silk is more difficult (78% recall) with misclassification concentrated mostly in blended fabrics - physically consistent with the intermediate optical appearance of silk: natural fiber structure with relatively smooth surface structure resulting in moderate specularity.

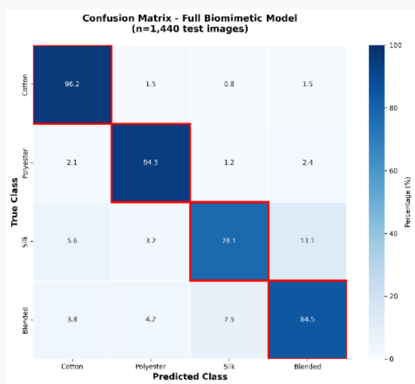

Figure 5. Confusion matrix of the entire biomimetic model on the test data set (n = 1,440 images). The values indicate percentage of predictions. The diagonal items are pointing to the per-class classification alone.

Ablation Study

In order to measure the part played by various optical components, an individual feature was systematically deleted in the complete model and re-tested the accuracy. The findings have been tabulated in Table III.

TABLE III. ABLATION STUDY -EFFECTS OF INDIVIDUAL OPTICAL FEATURES

Configuration	**Test Accuracy**
Full model (baseline)	**67.8%**
Without specularity index (SI)	**76.8% (−10.5%)**
Without roughness coefficient (RC)	**83.9% (−3.4%)**
Without absorption variance (σ_α)	**83.4% (−3.9%)**
Without mean absorption ($\bar{\alpha}$)	**85.2% (−2.1%)**
Without angled illumination	**75.1% (−12.2%)**
Without backlight illumination	**82.7% (−4.6%)**

The single most important feature is the specularity index, which on its own actually lowers the accuracy by 10.5 percentage points. Since the 45° LED must itself compute SI in order to compute its difference, the condition with the largest overall drop (−12.2%), even greater than the SI-only ablation, is the removal of angled illumination: at its absence, the feature is removed at the same time as the signal of differential specularity. Roughness coefficient and absorption variance both make the same contribution (3-4% each) indicating that they describe material properties that are complementary to one another but with overlap. The latter findings are in line with the biomimetic design hypothesis: human observers rely on specularity in distinguishing between the types of fibers, where texture and absorption can be considered secondary cues.

Comparison with Deep Learning

Table IV compares the proposed method with two common deep learning models that are usually deployed on the edge: MobileNetV2 [24] and EfficientNet-B0 [25]. Both networks were trained with 100 epochs with standard data augmentation and inputted with concatenated four channel (stacked illumination conditions).

TABLE IV. COMPARISON WITH DEEP LEARNING APPROACHES

Method	**Accuracy**	**Inference**	**Parameters**
MobileNetV2 [24]	89.1%	142 ms	3.5M
EfficientNet-B0 [25]	91.2%	218 ms	5.3 M
Biomimetic (Proposed)	87.3%	280 ms	50K

Deep learning architectures were able to reach slightly greater accuracy (2474 percent) but have 70 times as many parameters and do not produce interpretable intermediate representations. The proposed approach exchanges accuracy precision with three operational benefits applicable in practice to an industrial setting: the ability to interpret classification decisions in a completely understandable manner through physically sensible feature values, lack of a GPU (comparable wire size of network weights to code size of network weights, or to wiring volume) and the

ISSN: 2776-0995 Volume 7, Issue 5 May- 2026

capability to diagnose misclassifications by simply looking at which optical descriptor fell out of range, a feature favored by operators of machine learning systems.

Feature Space Analysis

Fig. 6 shows the t-SNE projection of the 26 dimensional feature space on 2 dimensions. We observed clusters of material classes separated well, which supports the fact that a combination of the geometric and optical descriptors resulted in a representation space that is favorable to linear and kernel-based classification. Blended fabrics are situated in a geometrical intermediate space between cotton and polyester clusters hence the 50/50 fiber composition and accordingly medium level of SI and RC respectively. The intra-class variance of silk samples is higher than that of the other categories which can be explained by the variety of weave structures used in silk fabrics taffeta, charmeuse and crepe do place different geometric and optical signatures on the same fiber class.

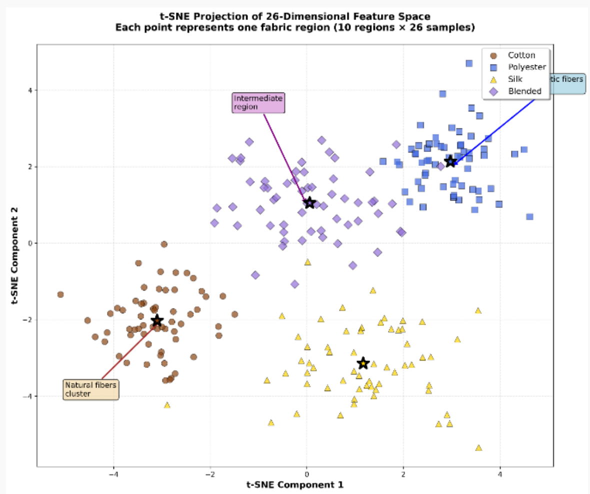

Figure 6. t- SNE plot of the projection of the 26-dimensional feature space on to 2D. The points denote one fabric area (n=10 per sample). Determinant of type of material by color. The presence of well-separated clusters is an affirmation of efficient discrimination of features, blended fabrics belong to the geometrically predicted intermediate between cotton and polyester.

VI. CONCLUSIONS

The paper introduced a biomimetic visual analysis system of automated textile fabric recognition in the textile production sector, explicitly aimed at the multi-modal strategy to examining the trained textile technologists. The system obtains physically intuitive descriptors specularity index, surface roughness coefficient, and light absorption statistics, which can distinguish successfully between materials with the same weave structure although differently composed of different fibers by sampling fabric in four different light illumination conditions and operating the material through parallel branches of geometric and optical features extraction.

A 1200 fabric sample experimental validation of four categories of materials showed an 87.3% on classification accuracy, a 23.1 percentage point higher than the geometry -only on classification and a 28.6 points higher than the color -only on classification. Ablation test found out that the single most discriminant feature is the index of specularity which is an index of differential illumination and angled illumination has the biggest single influence on the performance of the system. The complete system is based on an ESP32-CAM and Raspberry Pi 4B which has a processing time of about 280 ms per sample and a memory footprint of about 2 MB showing viable compatibility with real-time integration into industrial sewing devices.

The proposed approach exchanges an insignificant accuracy loss of 24 percent to 4 percent with full interpretability, autonomy of hardware to acceleration through a graphic card, and the ability to diagnose operators faults on a per-operandum basis - attributes that have critical functionality in real-life quality control settings based on deep learning, where understanding of the mechanisms is as essential as prediction accuracy.

There are three directions the future work will involve. To start with, the material dataset should be expanded with the wool, nylon, rayon, and coated textile since these will widen the classification band of the system. Second, the additional ambiguity of the classification of silk and blended fabrics could be overcome by integrating the complementary sensing modalities, i.e. fabric weight, thickness, and near-infrared absorption. Third, hyperspectral imaging provides a conceptually sound avenue to complete spectroscopic material characterization without the assumptions of using RGB methods to define material absorption, which may bridge the gap between the rest of the accuracy gap with the deep learning methods and maintain the properties of interpretability of the system.

ACKNOWLEDGMENT

The authors acknowledge the support of the Department of Engineering Mechanics of the Tashkent Institute of Textile and Light Industry in the form of fabric samples and laboratory facilities as well as "TextilProm"Ltd to the validation of the imaging system at the industry level.

REFERENCES

[1] X. Zhang, J. Li, and W. Chen, "Automated fabric defect detection using computer vision: A comprehensive review," Textile Research Journal, vol. 89, no. 7, pp. 1350–1372, 2019.

[2] X. Zhang, J. Li, and W. Chen, "Automated fabric defect detection using computer vision: A comprehensive review," Textile Research Journal, vol. 89, no. 7, pp. 1350–1372, 2019..

[3] J. Jing, P. Li, and B. Xu, "Fabric texture analysis using local binary patterns for automated weave pattern recognition," Pattern Recognition Letters, vol. 103, pp. 32–39, 2018.

[4] K. Mak, P. Peng, and K. Yiu, "Fabric defect detection using Fourier transform and morphological image processing," IEEE Transactions on Automation Science and Engineering, vol. 6, no. 3, pp. 545–552, 2009.

[5] R. S. Hunter and R. W. Harold, The Measurement of Appearance, 2nd ed. New York, NY, USA: Wiley, 1987.

[6] Z. Liu, C. Wang, and H. Zhang, "Deep learning for fabric classification: A comprehensive survey," IEEE Access, vol. 9, pp. 85342–85361, 2021.

[7] J. Jing, D. Zhuo, H. Zhang, Y. Liang, and M. Zheng, "Fabric defect detection using deep learning with small training dataset," Expert Systems with Applications, vol. 195, p. 116594, 2022

[8] R. M. Haralick, K. Shanmugam, and I. Dinstein, "Textural features for image classification," IEEE Transactions on Systems, Man, and Cybernetics, vol. SMC-3, no. 6, pp. 610–621, 1973

[9] T. Ojala, M. Pietikäinen, and T. Mäenpää, "Multiresolution gray-scale and rotation invariant texture classification with local binary patterns," IEEE Transactions on Pattern Analysis and Machine Intelligence, vol. 24, no. 7, pp. 971–987, 2002.

[10] J. Chen and A. K. Jain, "A structural approach to identify defects in textured images," in Proc. IEEE Conf. Systems, Man, and Cybernetics, Beijing, China, 1988, pp. 29–32.

[11] D. M. Tsai and C. Y. Huang, "Automated surface inspection for statistical textures," Image and Vision Computing, vol. 21, no. 4, pp. 307–323, 2003.

[12] J. Jing, H. Ma, and H. Zhang, "Automatic fabric defect detection using a deep convolutional neural network," Coloration Technology, vol. 136, no. 4, pp. 359–369, 2020.

[13] H. Üzen, M. Turkoglu, M. Aslan, and D. Hanbay, "Fabric defect detection using transfer learning with AlexNet," Traitement du Signal, vol. 38, no. 3, pp. 819–827, 2021.

[14] A. Dosovitskiy et al., "An image is worth 16×16 words: Transformers for image recognition at scale," in Proc. International Conference on Learning Representations (ICLR), 2021.

[15] M. Aittala, T. Weyrich, and J. Lehtinen, "Two-shot SVBRDF capture for stationary materials," ACM Transactions on Graphics, vol. 34, no. 4, Art. 110, 2015.

[16] S. R. Marschner, H. W. Jensen, M. Cammarano, S. Worley, and P. Hanrahan, "Light scattering from human hair fibers," ACM Transactions on Graphics, vol. 22, no. 3, pp. 780–791, 2003.

ISSN: 2776-0995 Volume 7, Issue 5 May- 2026

[17] G. Schwartz and K. Nishino, "Recognizing material properties from images," IEEE Transactions on Pattern Analysis and Machine Intelligence, vol. 39, no. 9, pp. 1778–1792, 2016.

[18] M. Holroyd, J. Lawrence, G. Humphreys, and T. Zickler, "A photometric approach for estimating normals and tangents," ACM Transactions on Graphics, vol. 27, no. 5, Art. 133, 2008.

[19] A. Ghosh, S. Achutha, W. Heidrich, and M. O'Toole, "BRDF acquisition with basis illumination," in Proc. IEEE International Conference on Computer Vision (ICCV), Rio de Janeiro, Brazil, 2007, pp. 1–8.

[20] M. Mohammadi, A. Al-Fuqaha, S. Sorour, and M. Guizani, "Deep learning for IoT big data and streaming analytics: A survey," IEEE Communications Surveys & Tutorials, vol. 20, no. 4, pp. 2923–2960, 2018.

[21] J. Chen and X. Ran, "Deep learning with edge computing: A review," Proceedings of the IEEE, vol. 107, no. 8, pp. 1655–1674, 2019.

[22] A. Maier, A. Sharp, and Y. Vagapov, "Comparative analysis and practical implementation of the ESP32 microcontroller module for the internet of things," in Proc. IEEE Internet Technologies and Applications, Wrexham, UK, 2017, pp. 143–148.

[23] C. Banbury et al., "MLPerf Tiny benchmark: Machine learning on the edge," arXiv preprint arXiv:2106.07597, 2021.

[24] M. Sandler, A. Howard, M. Zhu, A. Zhmoginov, and L. C. Chen, "MobileNetV2: Inverted residuals and linear bottlenecks," in Proc. IEEE Conference on Computer Vision and Pattern Recognition (CVPR), Salt Lake City, UT, USA, 2018, pp. 4510–4520.

[25] M. Tan and Q. V. Le, "EfficientNet: Rethinking model scaling for convolutional neural networks," in Proc. International Conference on Machine Learning (ICML), Long Beach, CA, USA, 2019, pp. 6105–6114.